Journal of Applied Polymer Science / Volume 139, Issue 4 / 51666

ARTICLE | Full Access

Thermoplastic polyurethanes for biomedical application: A synthetic, mechanical, antibacterial, and cytotoxic study

Rana Al Nakib, Antoniya Toncheva, Veronique Fontaine, Jérôme Vanheuverzwijn, Jean-Marie Raquez, Franck Meyer

First published: 20 September 2021
https://doi.org/10.1002/app.51666

Funding information: COST Action, Grant/Award Numbers: TD1305, CA15114; PROSTEM Project

Abstract

Thermoplastic polyurethanes (TPUs) bear tunable chemistry offering the possibility to develop a rich palette of physio-mechanical properties, making the materials suitable for various fields of application. The great variety in TPUs properties comes from the choices of the monomers and the reaction conditions. Herein, the mechanical properties of the developed TPUs are tailored, while fine-tuning the hard and soft segment molar ratio, as well as the reaction conditions. TPUs are synthesized from 4,4'-methylenebis(phenyl isocyanate), poly(tetrahydrofuran), and 1,4-butanediol, and their thermal and mechanical properties are fully characterized. The sample with the most appropriate mechanical properties that are suitable for catheter fabrication, is selected for the biomedical application. Quaternary ammonium salt is synthesized, and 0.5 mol% is incorporated in the TPU to confer antibacterial properties to the material while preserving its mechanical strength. The microbiological tests reveal the antibacterial effect of the developed materials against *Staphylococcus aureus* and *Pseudomonas aeruginosa*, as well as 80% SiHa cell viability, after 72 h of exposure, as part of the performed cytotoxicity studies. Finally, TPUs catheter prototypes fabrication is also proposed, applying an extrusion or injection molding approach for the production of biomedical devices with desirable mechanical properties.

1 INTRODUCTION

Polyurethanes (PUs) age back to the late 1930s when Otto Bayer and co-workers discovered their synthetic route from 1,6-diisocyanatohexane and 1,4-butanediol (BDO).[1] Nowadays, one of the most important applications of PUs is TPUs.[2, 3] TPUs are mainly synthesized from polyols and isocyanates producing alternating polymeric chains composed of soft polyol segments and

hard isocyanate segments. The soft parts form a continuous non-crystalline matrix and offer flexibility to the polymer due to their low glass transition temperature (T_g). In contrast, the hard segments, that is, diisocyanates and chain extenders, having a high T_g or melting temperature (T_m), offer stiffness as they tend to physically crosslink acting like fillers in the continuous matrix.[4] Therefore, TPUs bear unique chemistry which gave them a wide variation in their physical and mechanical properties making them suitable for many fields like automotive interior, the outer case of electronic devices, or transparent films.[5-7] Moreover, segmented PUs elastomers became among the most useful biomaterials in the biomedical field.[8-14] For instance, they are employed in fabricating blood bags, heart valves, vascular grafts, long and short-term implants, and cardiac pumps.[15-20] Among these medical devices, TPUs-based catheters represent an indispensable class of implantable biomaterials used in hospitals for the transfer of body fluids or administration of medication. However, these devices are also associated with healthcare-acquired infections (HAI), namely the development of infections while the patient is receiving care.[21-23] As a consequence, catheter bloodstream infections prolonged stays in hospitals and increase their associated costs.[24, 25] Therefore, the reduction of HAI attributable to the catheter can be achieved through the development of innovative devices endowed with antibacterial properties.

The most commonly used agents to exert antimicrobial effects are the quaternary onium salts, *N*-halamine, chitosan, peptides, antibiotics, nitric oxide, and metal ions.[26] As far as developing antibacterial TPUs is concerned, various active moieties have already been incorporated along with a segmented PU such as chloramphenicol,[27] cobalt,[28] or silver nanoparticles,[29] preventing thus adhesion/biofilm formation and spreading of bacteria.[30-34] Cationic agents are among the most frequently used antibacterial moieties when in contact with active surfaces, together with a potentially limited level of resistance development.[35] Specifically, positively charged quaternary onium salts are capable of disturbing/disorganizing the bacterial membrane through adsorption and penetration due to electrostatic interaction, leading to its damage. The alkyl chain length on these QOS was found to influence their antibacterial activity, where the longer the chain length (C_8 till C_{18}) the higher the antibacterial activity these QOS possess.[36] In this respect, Zanini et al. studied the effect of QAS-coated TPUs catheter through vapor phase plasma-induced graft polymerization of acrylic acid (AAc) against Gram-negative *Escherichia coli* and pointed to a 100% reduction of microorganism when compared with the untreated Pus.[37] QPS exhibits a similar mechanism of action to QAS but with a higher activity.[38] For instance, Gao et al. prepared water-insoluble composite particles PSt/SiO_2 coated with ammonium and phosphonium groups showing a strong antibacterial activity against *E. coli*.[39]

In light of these data, several strategies have been applied successfully to develop TPUs coating with good antibacterial properties. However, studies highlighting materials with good antimicrobial and mechanical properties and low cytotoxicity are scarce.[40] Limited research

works paid attention to understand the influence of the reaction conditions on the mechanical properties of the resulting materials.[41] Therefore, we decided to tackle this task through the determination of reaction conditions aiming at preparing TPUs with suitable mechanical properties for catheter application using conventional starting compounds, namely 4,4'-diphenylmethane diisocyanate (MDI) and BDO. Typically, commercial medical catheters like Elasthane™ or Biospan™ are composed of MDI that confers good mechanical properties although cariogenic aromatic amines can be released during a degradation process.[42] To address this issue, a purification procedure and cytotoxicity assessment will be performed. BDO is frequently used as a chain extender considering its beneficial behavior in enhancing the final mechanical properties of TPUs. Another important issue to be addressed is the achievement of acceptable TPUs melt processability that offers the possibility to produce catheters by solvent-free extrusion technology. In that work, the molar ratios, as well as the reaction conditions, were varied to study their influence on the TPUs properties. A series of samples were thereby studied comprehensively through thermal and mechanical characterization. Afterward, the formation of polymeric materials incorporating an active moiety will be implemented based on the compound showing the most promising physical features. To do this, we turned our attention towards a polymerizable quaternary ammonium salt (QAS) bearing a long alkyl chain group allowing its distribution along the polymer backbone. From a synthetic point of view, this method has the advantage to transpose the previous reaction process targeting the use of only 0.5 mol% of cationic species. This strategy is expected to maintain the mechanical properties whereas the QAS-containing TPU should demonstrate good antibacterial properties and low cytotoxic activities. Finally, TPUs catheter prototypes fabrication is also proposed, applying the extrusion approach.

2 EXPERIMENTAL

2.1 Materials

PTHF (1000 g/mol, Merck), MDI (250 g/mol, Alfa-Aesar), BDO (90.12 g/mol, Sigma-Aldrich), 3-bromo-1,2-propanediol 97% (Br-diol, 154.99 g/mol, Sigma-Aldrich), *N,N*-dimethyltetradecylamine (DMTDA, 241.46 g/mol, Sigma-Aldrich), and *N,N*-dimethyl formamide anhydrous (DMF, Sigma-Aldrich). Tryptic soy broth (TSB), fetal bovine serum (FBS), and Mueller-Hinton broth (MHB) were purchased from VWR. BDO was dried under vacuum for 3 h at 65°C before use and all the other materials were used as received without further purification.

2.2 Methods

2.2.1 Synthetic procedure of TPUs, QAS-C_{14}, and TPU-QAS-C_{14}

Synthesis of TPUs

1. TPU-1 and TPU-2 were prepared using the one-shot method. TPU-1 was synthesized from MDI (0.25 g, 1 mmol) and PTHF (1 g, 1 mmol) at 90°C whereas TPU-2 was synthesized from MDI (0.25 g, 1 mmol) and BDO (0.09 g, 1 mmol) at r.t., both reactions kept running for 4 h. TPU-3 to TPU-10 were synthesized following the prepolymer method, a two-step addition polymerization, except for sample TPU-6 where several steps were taken to add the starting compounds.
2. TPU-3: in the first step a reaction between MDI (0.5 g, 2 mmol) and PTHF (1 g, 1 mmol), was held for 2 h at 90°C. In the second step, BDO (0.09 g, 1 mmol) was added to the prepolymer and the reaction kept running for 3 h at r.t.
3. TPU-4: in the first step a reaction between MDI (1 g, 4 mmol) and PTHF (1 g, 1 mmol) was held for 2 h at 90°C. In the second step, BDO (0.27 g, 3 mmol) was added to the prepolymer and the reaction kept running for 3 h at r.t.
4. TPU-5: in the first step a reaction between MDI (1.15 g, 4.6 mmol) and PTHF (1 g, 1 mmol) was held for 2 h at 90°C. In the second step, BDO (0.27 g, 3 mmol) was added to the prepolymer and the reaction kept running for 3 h at r.t.
5. TPU-6: in the first step a reaction between MDI (0.5 g, 2 mmol) and PTHF (1 g, 1 mmol) was held for 2 h at 90°C. In the second step, BDO (0.09 g, 1 mmol) was added to the prepolymer and the reaction kept running for 0.5 h at 90°C. In the third step, MDI (0.55 g, 2.2 mmol) was added and the reaction kept running for 0.5 h at 90°C. In the final step, BDO (0.18 g, 2 mmol) was added and the reaction kept running for 0.5 h at 90°C.
6. TPU-7: in the first step a reaction between MDI (0.5 g, 2 mmol) and PTHF (1 g, 1 mmol) was held for 2 h at 90°C. In the second step, MDI (0.55 g, 2.2 mmol) and BDO (0.27 g, 3 mmol) were added to the prepolymer and the reaction kept running for 3 h at 90°C.
7. TPU-8: in the first step a reaction between MDI (0.5 g, 2 mmol) and PTHF (1 g, 1 mmol) was held for 2 h at 90°C. In the second step, MDI (0.55 g, 2.2 mmol) and BDO (0.27 g, 3 mmol) were added to the prepolymer and the reaction kept running for 3 h at 80°C.
8. TPU-9: in the first step a reaction between MDI (0.55 g; 2.2 mmol) and PTHF (1 g; 1 mmol) was held for 2 h at 90°C. In the second step, MDI (0.5 g, 2 mmol) and BDO (0.27 g, 3 mmol) were added to the prepolymer and the reaction kept running for 3 h at 90°C.
9. Typical procedure: TPU-10 was prepared by reaction of PTHF/MDI/BDO in a molar ratio of 1/4.4/3, respectively. The synthesis was carried out at 90°C in a 250 ml 2-neck round bottom flask equipped with a magnetic stirrer and a nitrogen inlet. In the first step, PTHF (1 g; 1 mmol) and DMF (10 ml; 25% wt/vol) were introduced into the flask and kept for 10 min before adding MDI (0.55 g; 2.2 mmol) dropwise where the reaction continued for 2 h at 90°C. In the second step, BDO (0.27 g; 3 mmol) and MDI (0.55 g; 2.2 mmol) were added to the mixture, the reaction was kept at 90°C for 3 h.

At the end of the reaction, the viscous solution was dried in a ventilated oven overnight at 60°C, followed by 12 h of drying in a vacuum oven at 60°C. For purification, Soxhlet extraction was

performed for 48 h at 40°C using chloroform, as a solvent. Solvent casting was applied to obtain the films through dissolving the samples in DMF.

The yield percentage was calculated for all the reactions using the weight of materials recovered after Soxhlet extraction divided by the weight of starting compounds.

Size exclusion chromatography was performed in DMF at 50°C using an Agilent liquid chromatograph equipped with an Agilent degasser, an isocratic HPLC pump (flow rate = 1 ml/min), an Agilent autosampler (loop volume = 100 µl, solution concentration = 1 mg/ml), an Agilent-DRI refractive index detector and three columns: a PL gel 10 µm guard column and two PL gel Mixed-D 10 µm columns (linear columns for the separation of MWPS ranging from 500 to 107 g/mol). Polystyrene standards were used for calibration.

TPU-4: ^{1}H-NMR (500 MHz, THF-d_8, δ): 8.58 (s, 1H, –NHC=O), 7.37–7.04 (m, 1H, Ar H), 4.11 (m, 2H, $COOCH_2$), 3.82 (s, 2H, Ar CH_2 Ar), 3.36 (m, 2H, –CH_2–O), 1.57 (m, 2H, –CH_2).

Synthesis of N-(2,3-dihydroxypropyl)-N,N-dimethyltetradecan-1-aminium bromide (QAS-C_{14})

Br-diol (0.186 g, 1.2 mmol) and DMTDA (0.24 g, 1 mmol) were stirred in refluxing ethanol at 80°C for 48 h. Then, the solution was cooled down and the compound was precipitated using diethyl ether, filtered, and dried giving QAS-C_{14} (396.46 g/mol) with a yield of 80%.

^{1}H-NMR (500 MHz, $CDCl_3$, δ): 3.5–3.81 (m, 6H, –CH_2–), 3.35 (s, 6H, N-CH_3), 1.75 (m, 2H, –CH_2–), 1.25 (m, 22H, –CH_2–), 0.87 (t, J = 6.8 Hz, 3H, –CH_3).

Synthesis of TPU-QAS-C_{14}

TPU-QAS-C_{14} was prepared by reaction of PTHF/MDI/BDO/QAS-C_{14} with molar ratios of 1/4.4/2.96/0.04, respectively. The synthesis was carried out at 90°C in a 250 ml 2-neck round bottom flask equipped with a magnetic stirrer and a nitrogen inlet. In the first step, PTHF (1 g; 1 mmol) and DMF (10 ml; 25% wt/vol) were introduced into the flask and kept for 10 min before adding MDI (0.55 g; 2.2 mmol) dropwise where the reaction continued for 2 h at 90°C. In the second step, BDO (0.265 g; 2.95 mmol), MDI (0.55 g; 2.2 mmol), and QAS-C_{14} (15 mg; 0.04 mmol) were added to the mixture, the reaction was kept at 90°C for 3 h. For purification, Soxhlet extraction was performed for 48 h at 40°C using chloroform, as a solvent.

^{1}H-NMR (500 MHz, DMSO-d_6, δ): 9.5 (s, 1H, –NHC=O), 8.5 (s, 1H, –NHC=O), 7.33, 7.07 (m, 2H, Ar H), 4.09 (m, 2H, $COOCH_2$), 3.88 (s, 2H, Ar-CH_2-Ar), 3.4 (m, 1H, –CH–), 3.35 (m, 2H, O-CH_2), 1.69–1.48 (m, 2H, CH_2), 1.29 (m, 2H, CH_2) 1.17–0.85 (m, 3H, CH_3).

2.2.2 Characterization methods

^{1}H-NMR

^{1}H-NMR spectra were recorded on a BrukerAVII-500 MHz spectrometer. Spectra were obtained for solutions of approximately 20 mg in 0.6 ml of THF-d_8, DMSO-d_6, or $CDCl_3$.

FT-IR

FT-IR spectra were measured with spectrometer model 4100 Perkin Elmer over a wavenumber range 500–4000 cm^{-1} and 32 scans.

TGA

TGA of TPUs was evaluated by TGA Q500, TA Instruments. The samples were analyzed (5–10 mg) over the temperature range of 25–600°C at a heating rate of 10°C/min under N_2 atmosphere.

MDSC

MDSC analysis was carried out on a TA instrument DSC-Q200. The detailed method was as the following: equilibrate at −80°C, data storage on, modulate ±1°C every 60 s, ramp 10°C/min to 250°C, mark end of cycle 0, modulate ±1°C every 60 s, ramp 10°C/min to −80°C, mark end of cycle 1, modulate ±1°C every 60 s, ramp 10°C/min to 250°C, mark end of cycle 2. The DSC data are presented after the second scan.

DMTA

DMTA was performed on a DMTA Q800 analyzer, using a 0.13 mm thick, 5 mm wide, and 4.8 mm long rectangular specimen. Curves displaying storage modulus (E'), loss modulus (E''), and the loss factor (tan δ) were recorded in the range of −80 to 175°C at a heating rate of 3°C/min. Frequency of 1 Hz and displacement of 20 μm were used.

Mechanical analysis

Tensile strength, Young's Modulus, and elongation at break of polymer films with a dog-bone shape were measured on Zwick at a crosshead speed of 25 mm/min at room temperature (RT). Samples were conditioned for 48 h in a vacuum oven at 60°C before performing the analysis. The thickness and width of the specimens were 1.3 and 4 mm, respectively. The length of the sample between the two mechanical grips of the testing machine was 10 mm. Five measurements were conducted and the results were averaged to get a mean value.

Contact angle

Wettability evaluations were conducted by Tensiometer DSA10 Mk2 to measure the contact angle. A water droplet of 10 μl was discharged through a micrometer syringe on the surface of the polymer. Images of the droplet were captured after allowing it to spread for 10 s. Five sets of measurements were taken to narrow down the error percentage.

SEM

SEM of the samples was performed after cryofracturing them and coated with a gold nanolayer by a sputtering technique.

2.2.3 Biological tests

Antibacterial activity assessment of compounds

The anti-bacterial activity of QAS-C_{14} was evaluated against both Gram-positive *Staphylococcus aureus* (ATCC 6538) and Gram-negative *Pseudomonas aeruginosa* (ATCC 15442) bacteria by the broth microdilution method. This was performed in sterile 96-well plates inoculated with 100 µl/well sterilized Mueller Hinton broth. Using a 2.5 mg/ml initial concentration of the active moiety in the first well, we further diluted the compound by two-fold serial dilutions in the 96-well plate. Then, 100 µl of diluted bacteria (3×10^6 cells/ml) were added to each well. As negative controls, two to three wells on each plate were without any active moiety. The minimal inhibitory concentration (MIC) of the tested compounds were interpreted by visual inspection of the bacteria culture plate after 24 h incubation at 37°C.

Contact antibacterial activity of polymers

Films of 20 mm diameter and 1 mm thickness were sterilized under UV light (in the range 200–280 nm) for 30 min and placed in a well of a 12-well plate. Copper coin and TPU-10 were used as the positive and negative control, respectively. *S. aureus* (ATCC 6538) and *P. aeruginosa* (ATCC 15442) strains were cultured in the nutrient broth agar, grown overnight at 37°C. To prepare the inoculum, 1 Mc Farland turbidity in peptone water was prepared and diluted 1/500 in biofilm stimulating medium, TSB/NaCl for Gram-positive and brain heart infusion (BHI)/glucose for Gram-negative. The assay was performed using 5 min. Transient contact with the inoculum present on sterile compress placed in a petri dish. Then the surfaces were removed and placed, face turned, in the well, and kept to dry for 10 min. Finally, 1 ml biofilm stimulating medium was added and the wells were incubated for 24 h at 37°C. Serial dilutions of the surviving microorganisms were done after the incubation, with the first dilution done in an inactivating solution and the next ones in buffered peptone water. 1 ml of each dilution was seeded in tryptic soy agar. After incubation, the colony-forming units (CFU) were counted to assess eventual survivor log reduction after contact with the surface. All the reported experiments were repeated at least three times.

Cytotoxicity assessment of dissolved polymers

A 3-(4,5-dimethylthiazol-2-yl)-2,5-diphenyltetrazolium bromide (MTT) assay was carried out to examine the cytotoxicity of the dissolved polymers.[43] A 100 µl epithelial human cell line, SiHa, (10^5 cells/ml) in 10% fetal bovine serum (FBS) Dulbecco's Modified Eagle Medium (DMEM) were seeded in each well of a 96-well plate, filled with 100 µl medium culture, and incubated at 37°C

for 24 h in the presence of 5% carbon dioxide. The initial concentration of the DMSO dissolved polymers (previously sterilized by 24 h incubation in 75% ethanol) varying from 0.125 to 32 µg/ml, was further diluted on a 96-well plate and added to the adherent SiHa monolayer cells for further incubation at 37°C. After 24 h, the MTT was added to each well (0.5 mg/ml final concentration) and the culture plate was further incubated for 5 h at 37°C. Then, the culture medium was removed, cells were washed with phosphate buffered saline (PBS) and the insoluble formazan crystals were dissolved in 100 µl/well DMSO by shaking the plates for 15 min. at r. t. The absorbance was measured at 570 and 630 nm using a microplate reader (Bio-Rad 680) after shaking the plates for 15 min. The results were expressed as the percentage of optical density (OD) relative to the OD from the control cells, without compounds, set up to 100% viability. The assays were performed in triplicate in three separate experiments. The IC_{50} range, defined as the tested concentrations that reduce the global cell growth by 50%, was used as the parameter of the anti-proliferative effect compared to the control condition. The IC_{50} value was calculated using the following equation:

$$IC_{50} = [(X_2 - X_1)(50 - Y_1)/(Y2 - Y1)] + X_1$$

where X_1 is the higher dissolved polymer concentration that borders the concentration reducing the global cell growth by 50%, X_2 is the lower dissolved polymer concentration that borders the concentration that reduces the global cell growth by 50%, Y_1 means the percentage of viable cells at the X_1 concentration and Y_2 is the percentage of viable cells at the X_2 concentration.[44]

Cytotoxicity assessment of polymers

Specimens (5, 6, and 1.5 mm) were immersed in the 10% FBS DMEM and pre-incubated for 24 h at 37°C in the presence of 5% carbon dioxide. SiHa cells were seeded in 24-multiwell plates (6×10^4 cells/well) in 500 µl 10% FBS DMEM and incubated for 24 h at 37°C. Then, the growth medium was replaced with 2% FBS DMEM and polymers (retrieved from the pre-incubation culture medium) were carefully placed directly on the cell monolayer (method following ISO 10993-5).[45] Cells cultured in wells without polymers served as controls. After 24, 48, or 72 h incubation at 37°C in the presence of 5% carbon dioxide, an MTT colorimetric assay was performed to evaluate cell viability. Briefly, the culture medium and specimens were removed with great care. Then, adherent cells were rinsed once with phosphate-buffered saline (PBS) before adding 500 µl per well of MTT solution (1 mg/ml in 10% DMEM). The plates were then returned to 37°C. After 3 h incubation, plates were centrifuged for 10 min, MTT solution was removed and formazan crystals formed in live cells were dissolved by adding 500 µl/well DMSO. The absorbance was measured at 570 and 630 nm using a microplate reader (Bio-Rad 680)

after shaking the plates for 15 min. The results were expressed as the percentage of OD relative to the OD from the control cells, without polymers, set up to 100% viability. The assays were performed in triplicate in three separate experiments.

2.2.4 Catheter prototyping

A series of catheter fabrication was proposed through extrusion, using Process 11 parallel twin-screw extruder. The obtained TPUs were introduced in the third introduction zone, to reduce the temperature exposure of the TPUs and reducing the probability of thermal oxidation of the polymer matrix. The working temperature was 200°C with a crew speed of 15 rpm, for the production of regular filament with a diameter of 2.5 mm and length of several tens of centimeters. Subsequently, the filament was subjected to perfusion with a vertical drill to create a series of catheters with different lengths and an inner diameter of 1.07 mm. A customized injection molding approach was also proposed, for fast single catheter production with various inner diameters. The catheter morphological characteristics were studied by scanning electron microscopy (SEM, SEM Philips XL20).

3 RESULTS AND DISCUSSION

3.1 Synthetic procedure of TPUs

In the present study, series of TPUs were synthesized following the two-step polyaddition method as presented in Figure 1, except for TPU-1 and TPU-2 which followed the one-shot method. TPU-1 and TPU-2 were held to study the reactivity of BDO and PTHF with MDI and to analyze the influence of the soft segment and the chain extender on TPUs physical properties. TPU-1 resulted in a soft and sticky material reflecting no phase separation between the two segments due to the lack of a chain extender.[46] TPU-2, on the other hand, resulted in a brittle material and low molecular weight, 14 kDa, due to the lack of a soft segment. The rest of the polymers were prepared through the formation of a prepolymer using a different molar ratio of PTHF, BDO, and MDI. When comparing the molecular weight of the synthesized TPUs, it was noticed that excess in the MDI is required in both steps to increase the M_n from 10.8 kDa, TPU-3, to 38 kDa, TPU-10. The temperature variation was also studied where the temperature of 90°C gave the most convenient yields and molecular weights, where TPU-8 that was processed at 80°C gave a low molecular weight of 15 kDa.

FIGURE 1

Polyaddition two-step method for the synthesis of TPUs [Color figure can be viewed at wileyonlinelibrary.com]

From these reactions, it was noticed a good conversion in final polymeric materials since yields were in the range of 72%–91% (Table 1). All the samples were transparent, except for TPU-9 which appeared to be opaque, and they were all soluble in DMSO, THF, and DMF. Depending on the materials composition, TPUs have different physical aspects: TPU-1 presents soft and sticky behavior, TPU-2 is brittle, TPU-3, 8, and 9 are soft, TPU-4, 5, 6, 7 are rigid, and TPU-10 is elastic.

TABLE 1. TPUs monomer composition and monomer molar ratio, TPUs synthesis working temperature, reaction yield, molecular weight (M_n), dispersity (Đ), and images

Code	TPUs composition MDI/PTHF/BDO (molar ratio)			Temperature (°C)		Yield (%)	M_n (kDa)	Đ	Images
	MDI	PTHF	BDO	First step	Second step				
TPU-1	1	1	0	90		72	21	1.7	Soft, sticky
TPU-2	1	0	1	r.t.		77	14	6.4	Brittle
TPU-3	2	1	1	90	r.t.	91	10.8	1.6	Soft
TPU-4	4	1	3	90	r.t.	90	21	5.5	Rigid
TPU-5	4.6	1	3	90	r.t.	89	27	1.8	Rigid
TPU-6	4.2	1	3	90	90	90	25	2.4	Rigid
TPU-7	4.2	1	3	90	90	91	24	2	Rigid
TPU-8	4.2	1	3	80	80	88	15	2	Soft
TPU-9	4.2	1	3	90	90	87	13	1.4	Soft
TPU-10	4.4	1	3	90	90	90	38	2	Elastic

Segmented PUs can be obtained by a step-growth polymerization following a one-shot method or the prepolymer method.[47, 48] In the one-shot method, the isocyanate, polyol, and chain extender react together whereas in the prepolymer method the polyol first reacts with an excess of isocyanate giving a functional prepolymer. This functional prepolymer subsequently participates in the chain extension with a chain-extender, resulting in a segmented copolymer of well-defined structure and controlled properties by comparison with the one-shot method.[49-51] The prepolymer method offers a structural regularity in the produced PU leading to a better packing of the hard segments. Hence, when high mechanical properties are needed the prepolymer method is adopted. Additionally, chain extenders are used in PUs to increase the length of the hard segment and thus the molecular weight of the material.[52] The chain extender has a huge influence on the final material of PUs, specifically on their mechanical properties.[53]

Aliphatic or aromatic isocyanates are currently used in the design of biomedical PU grades.[54] Aromatic diisocyanates, particularly MDI, are the most popular biomedical applied ones.[55] It was proven that MDI-based PUs give a better phase separation and higher hydrogen bonding density, leading to higher mechanical properties and thermal stability when compared to toluene diisocyanate (TDI)-based Pus.[56] Alternatively, aliphatic diisocyanates are commonly used to make degradable PUs with low toxicity issues, but they provide lower mechanical properties compared to their aromatic counterparts.[57] In this respect, the most commonly used aliphatic diisocyanates include 1,4-butane diisocyanate (its hydrolyzed product is putrescine, naturally occurring in the body), 1,6-hexamethylene diisocyanate (HMDI), and lysine diisocyanate (yield safe carboxylic byproduct). The reactivity of R-NCO depends on the nature of R, as the electrophilicity of the isocyanate follows the sequence phenyl > benzyl > n-alkyl > cyclohexyl. Poly-functional isocyanates, having more than two–NCO groups also exist, such as triphenylmethane triisocyanate, which attracted a lot of attention in the coating and adhesive industries.[58] Morales et al. studied 3 polyisocyanates, L-lysine ethyl ester diisocyanate (LDI), pentamethylene-diisocyanate (PDI) isocyanurate trimer, and hexamethylene-diisocyanate (HDI) allophanate as the isocyanates to produce bio-based thermosetting PUs with T_g values ranging from −41 to +21°C and thermal stabilities of up to 300°C.[59] However, in our study, MDI was used to produce thermoplastic polymers and purification was done to remove all starting materials from the final material to ensure safety in the produced TPUs. Additionally, Tarng et al., reported the thermal degradation of MDI-based segmented PUs using thermogravimetric analysis, ultraviolet–visible spectroscopy, GPC, and FTIR spectroscopy.[60] The study confirmed the safety of using MDI in PUs for biomedical applications as no cleavage of N-H and C-H bonds on the hard segment were detected below 200°C.

3.2 Characterization methods

GPC study revealing the M_n of all the samples is presented in Figure 2. A considerable

fluctuation in the M_n was observed between the samples with TPU-10 having the highest value (38 kDa). Through analyzing these values, few remarks on the synthesis conditions are worth mentioning. Missing one of the starting materials led to a low M_n, as in the case of TPU-1 and TPU-2. Additionally, a slight increase in the reaction temperature from 80 to 90°C induced a dramatic increase of M_n from 15 to 24 kDa, as seen for TPU-8 and TPU-7, respectively. An excess of MDI also appeared to be crucial in maintaining a high M_n. Under the same conditions, TPU-4 was recovered with a molecular weight twice as high as TPU-3, using the double amount of isocyanate derivative in the prepolymer preparation step. Therefore, to obtain a high M_n of TPUs, the prepolymer formation should be prepared with PTHF and MDI at a temperature not below 90°C, using an excess of MDI considering the high sensitivity to water which may lead to its inactivation.[61]

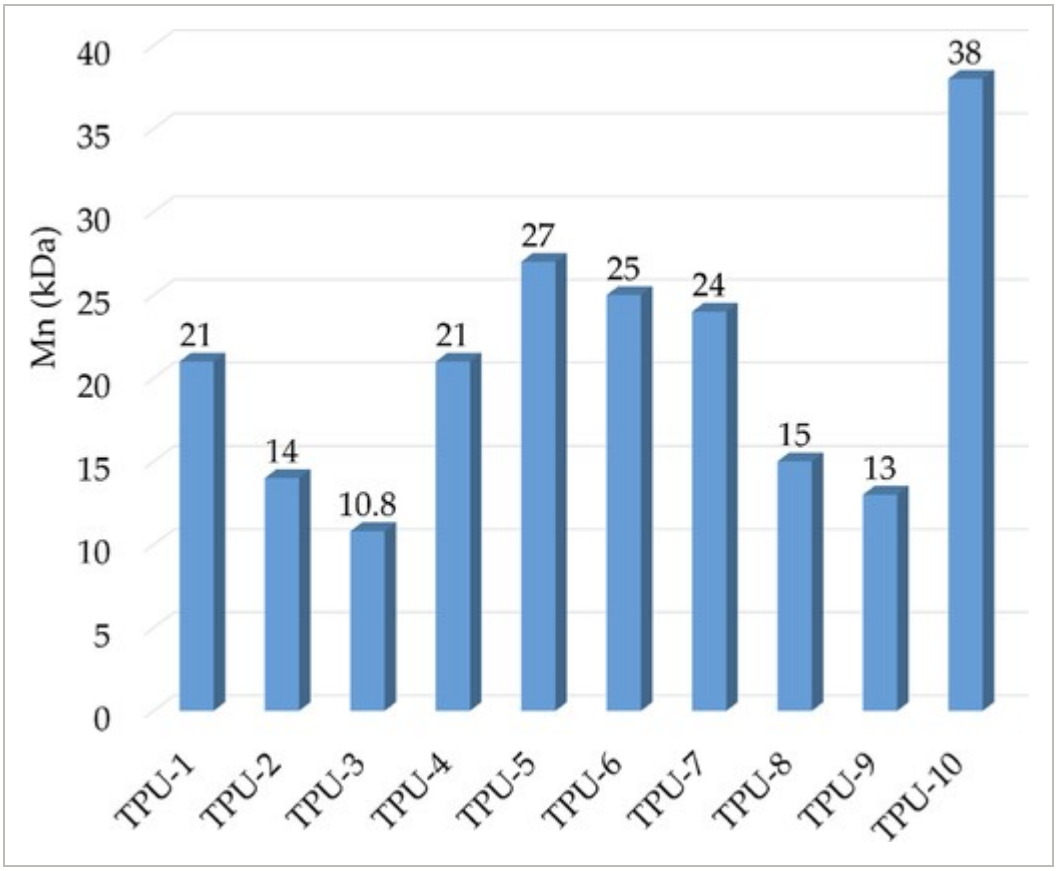

FIGURE 2

Open in figure viewer | PowerPoint

M_n of the synthesized TPUs [Color figure can be viewed at wileyonlinelibrary.com]

TPUs syntheses were monitored by FT-IR spectroscopy (Figure 3). All spectra produced almost the same characteristics, the N–H stretching bands were observed at 3300 cm^{-1} while the medium-strong band at 1600 cm^{-1} represents the bending vibrations of N–H. Stretching vibration of C=O was observed around 1730–1700 cm^{-1}, whereas typical signals for aromatic

rings are around 1700–1500 cm^{-1} (C=C stretching vibration) and bands in the region 900–700 cm^{-1} belong to out-of-plane bending vibration of C-H in multi-substituted benzene rings. Furthermore, the bands observed at around 1530 and 1450 cm^{-1} correspond to C–N, supporting the formation of the urethane linkage and confirming the successful polymerization.[62] In addition, the C–H stretches assigned to the CH_2 groups of PTHF and BDO are found in the region 2940–2850 cm^{-1} and the broad and strong peak at 1100 cm^{-1} corresponds to the C–O–C ether bond. Finally, the full conversion of the NCO groups is proved by the absence of the band at 2270 cm^{-1}.[63]

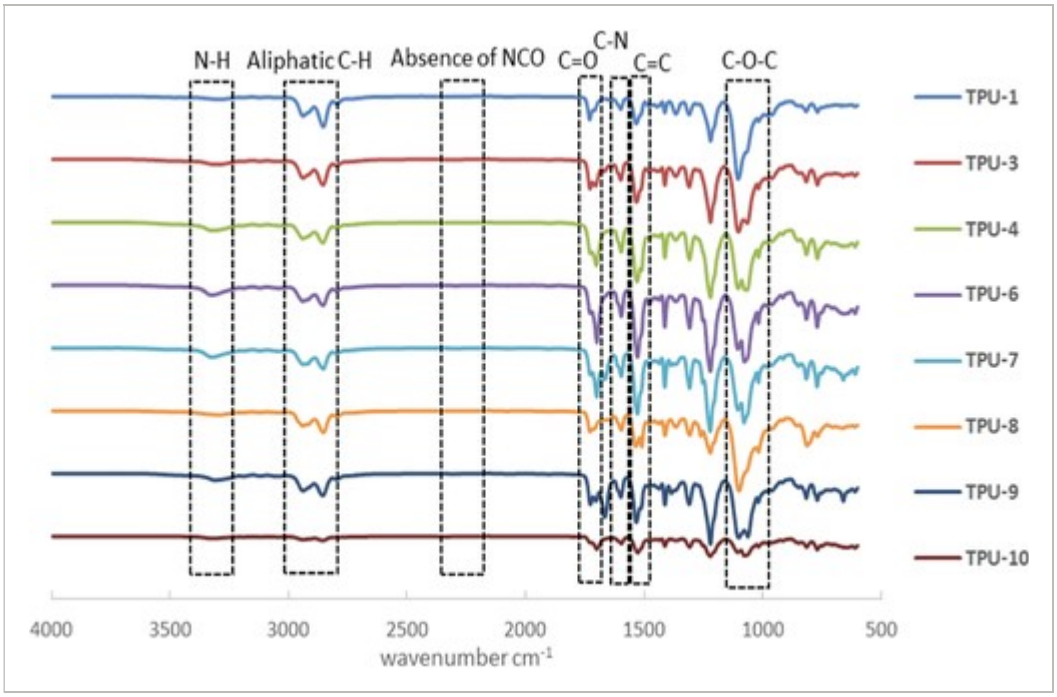

FIGURE 3

Open in figure viewer | PowerPoint

FT-IR spectra of the synthesized TPUs [Color figure can be viewed at wileyonlinelibrary.com]

Further ^{1}H-NMR spectra of the synthesized TPUs corroborated the formation of the urethane functionality through the presence of typical peaks at 8.58 and 4.12 ppm assigned to the N–H and CH_2–O bonds, respectively (Figure 4 and Figure S1). Moreover, the purification by Soxhlet extraction using chloroform for 48 h appeared to be effective, as highlighted by the absence of starting materials.

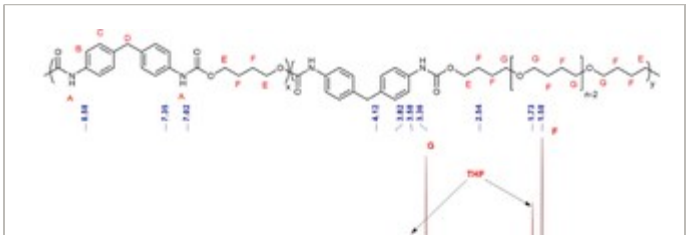

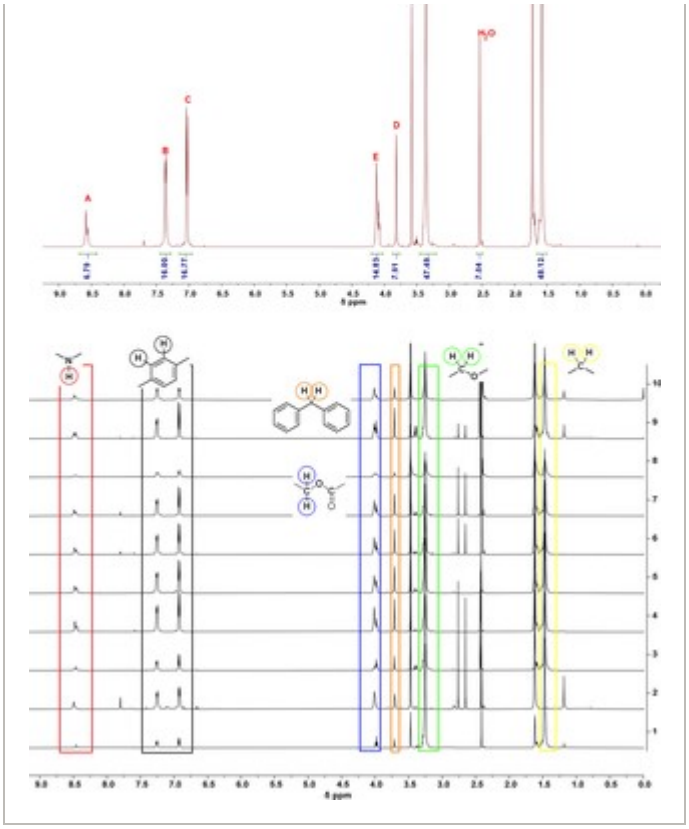

FIGURE 4

Open in figure viewer | PowerPoint

^{1}H-NMR in THF-d_8 of TPU-4 (top). ^{1}H-NMR with the main characteristic peaks of the synthesized TPUs (bottom) [Color figure can be viewed at wileyonlinelibrary.com]

The thermal stability of synthesized TPUs was examined via TGA from r.t. to 600°C (Figure S4). It appeared that the decomposition occurred in a two-step process for all materials. At approximately 320°C, the degradation of the urethane bonds was seen, whereas the destruction of the ether bonds took place around 415°C.[64] All the samples were thermally stable up to 260°C with a mass weight loss of less than 3%.

The thermal transformation of the synthesized TPUs was also analyzed using the MDSC. A T_m of the hard segment crystals was observed in the range of 170 and 200°C with a broad endothermic peak due to the microphase separation structure of the samples. An exception was TPU-1 lacking the chain extender and TPU-2 lacking the soft segment, as mentioned before. The T_m of TPU-7 and 10 was broad and lower in intensity, this could be explained by the lower crystallinity in these samples. As for the T_g of the soft segment, it was observed between −35 and −48°C except for TPU-1, 2, and 6. The absence of the T_m in TPU-1 is again due to the absence of the chain extender; however, a T_g was observed around 8°C corresponding to the soft segment. As far as TPU-2 was concerned, a T_g was found at 105°C which was expected taking into consideration how brittle this sample was. A drastic decrease in the M_n due to the

absence of PTHF which led to short polymer chains decreased the mobility of the sample giving a high T_g value. Whereas TPU-6 showed a T_g around −26°C, this shift in T_g was due to the interruption in adding the starting compounds while synthesizing (Figure S4).

The melting enthalpy was also measured and presented in Table 2. The values show a significant variation between the samples. This can be explained by the variation of the hard segment amount in the polymers responsible for the melting behavior of the samples.[65, 66] For sake of clarity the melting transition, particularly in the case of the TPUs presenting low melting enthalpy, was confirmed using the reversible part of the MDSC analysis in which endothermic phenomena were observed and related to the melting.

TABLE 2. Thermal analysis values of the synthesized TPUs

Samples	T_o (°C)	T_d (°C)	T_g (°C)	T_m (°C)	ΔH (J/g)
TPU-1	280	348/405	8	—	—
TPU-2	300	360/404	105	—	—
TPU-3	260	340/408	−36	171	2.02
TPU-4	262	339/414	−41	190	25.8
TPU-5	276	308/414	−37	195	18.9
TPU-6	266	311/414	−26	195	13.1
TPU-7	290	348/418	−38	200	10.7
TPU-8	265	312/426	−42	178/211	6.9
TPU-9	220	302/412	−48	188	19
TPU-10	254	273/419	−35	189	1

Note: T_o, onset of weight loss; T_d, degradation temperature; T_m, melting temperature; ΔH, melting enthalpy.

DMTA was used to study the viscoelastic behavior (the thermal transition of the soft and hard microdomain) of the newly prepared samples TPU-4 to TPU-10, the other samples were either too soft or too brittle to examine. The temperature dependence of the storage modulus, the loss modulus, tan δ, and their corresponding values are illustrated in Figure 5. A transition after −50 and 150°C was observed in all the samples that correspond to the T_g (matching with the

MDSC results) and the melting (of hard segment crystals), respectively. This transition is typical in TPUs where many studies on similar material experienced the same results.[67, 68] All samples showed a high rubbery plateau between these two transitions reflecting a high elasticity supported by the physical cross-linking. Tan δ represents the ratio of the viscous to elastic response of the viscoelastic TPUs and measures the energy dissipation of the material. The height and area under the tan δ curve indicate the total amount of energy that can be absorbed by the material.[69] It is noticed that all the samples had the same low tan δ values reflecting their elasticity and the low miscibility between the flexible segments and the rigid ones revealing phase separation.[70, 71]

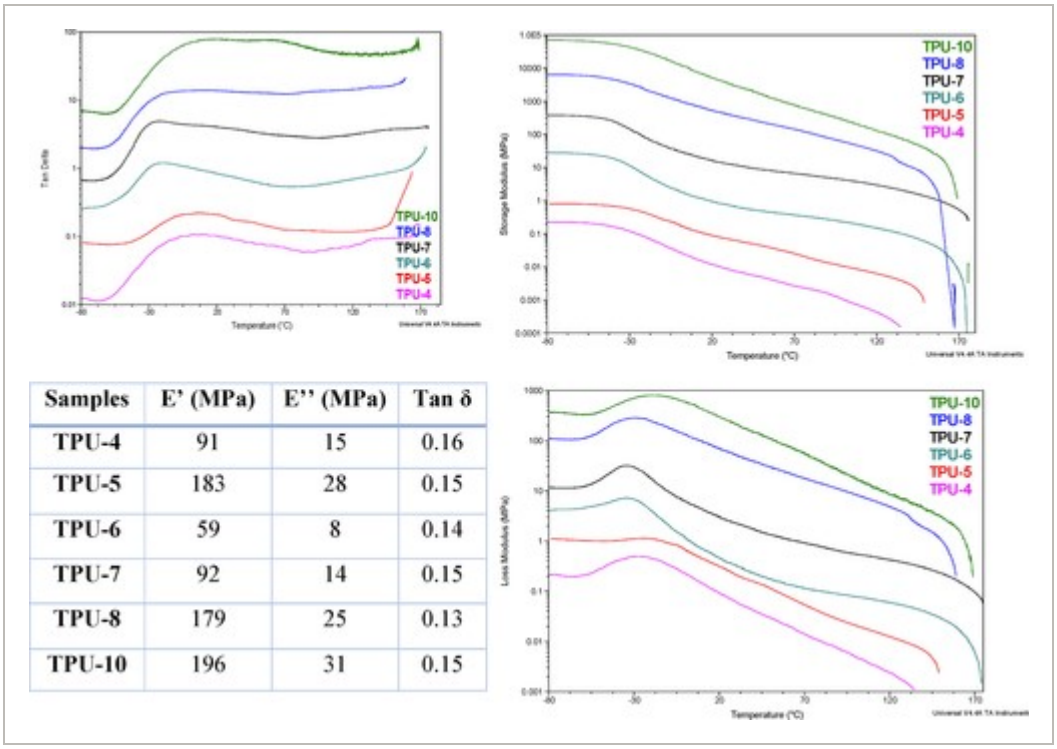

Samples	E' (MPa)	E'' (MPa)	Tan δ
TPU-4	91	15	0.16
TPU-5	183	28	0.15
TPU-6	59	8	0.14
TPU-7	92	14	0.15
TPU-8	179	25	0.13
TPU-10	196	31	0.15

FIGURE 5

Open in figure viewer | PowerPoint

DMTA analyses of TPU-4 to TPU-10: Tan δ (top left), storage modulus (top right), loss modulus (bottom right), and E' (storage modulus), and E" (loss modulus) at 37°C [Color figure can be viewed at wileyonlinelibrary.com]

Stress–strain curves of TPU-4 to TPU-10 are also illustrated in Figure 6, considering that the other samples were not tested due to their poor physical properties. It was noticed that the results are in line with GPC values. The samples with the highest M_n had the highest tensile strength and storage modulus. Thanks to the excess of MDI while synthesizing these samples (TPU-10 and TPU-5) which assured a high hard segment content with NCO terminals leading to the physical crosslinking through H-bonding. As for the ductility, a decrease was observed in the samples synthesized at lower temperatures, as in the case of TPU-4 and TPU-8.

Comparable results were obtained in a study where TPUs were synthesized using an increasing molar ratio of MDI.[72] It confirms that an increase in the hard segment leads to higher mechanical properties. In a study by Bovas et al., several TPUs samples were synthesized for medical catheter fabrication, and their mechanical properties revealed comparable values to this study, where the tensile strength was between 37 and 44 MPa for untreated catheters and between 17 and 25 MPa for the chemically aged ones.[73]

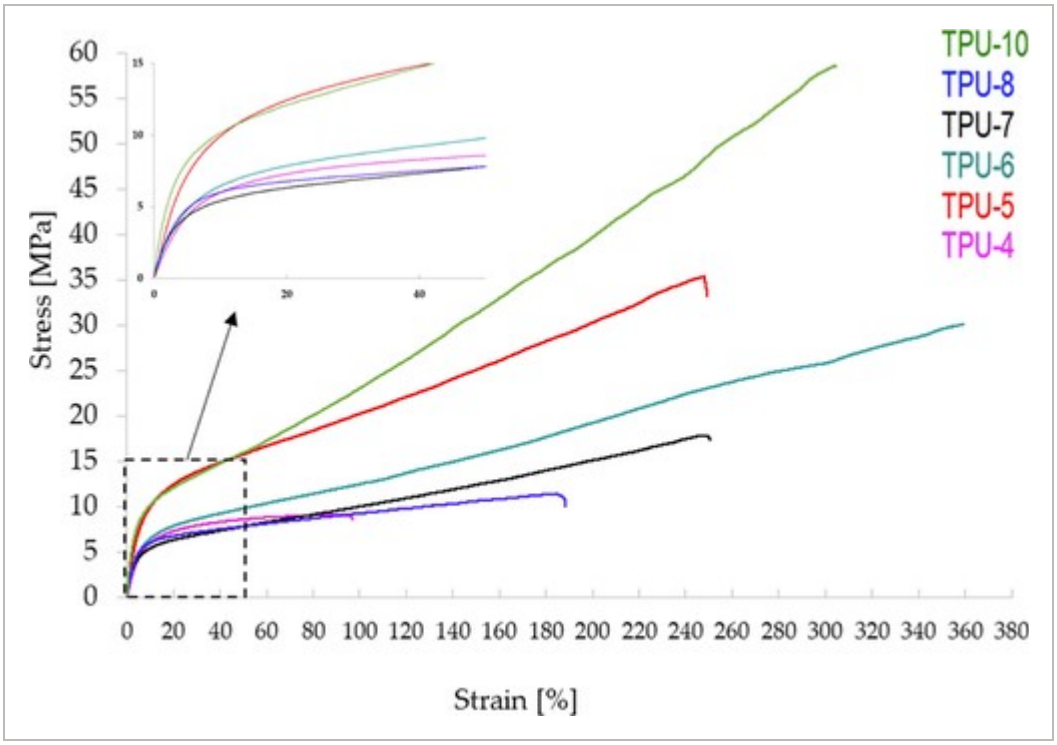

FIGURE 6

Open in figure viewer | PowerPoint

Stress–strain curves of the synthesized TPUs [Color figure can be viewed at wileyonlinelibrary.com]

Conclusively, TPU-10 was noticed to have the most convenient characteristics, in terms of mechanical strength that has convinced us to prepare a new compound endowed with antibacterial properties targeting a biomedical application.

3.3 Synthetic procedure of QAS-C_{14}

As a proof of concept, a TPU possessing a QAS unit was synthesized and tested for its antibacterial property and cytotoxicity as a potential catheter design. For this, a QAS bearing a long alkyl chain was selected, considering the potential interaction between the cationic ammonium part with the negatively charged bacterial cell wall, and the ability of the aliphatic group to disrupt the peptidoglycan structure organization. QAS-C_{14} was thereby selected as polymerizable salt. This compound was obtained in an 80% yield through the quaternization of

nitrogen of DMTDA and Br-diol (Figure 7). A ^{1}H-NMR analysis confirmed the successful quaternization (Figure S2).

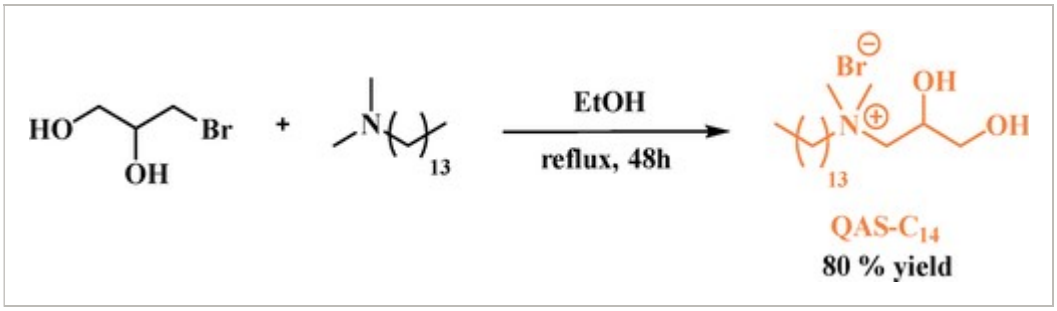

FIGURE 7

Open in figure viewer | PowerPoint

QAS-C_{14} synthesis [Color figure can be viewed at wileyonlinelibrary.com]

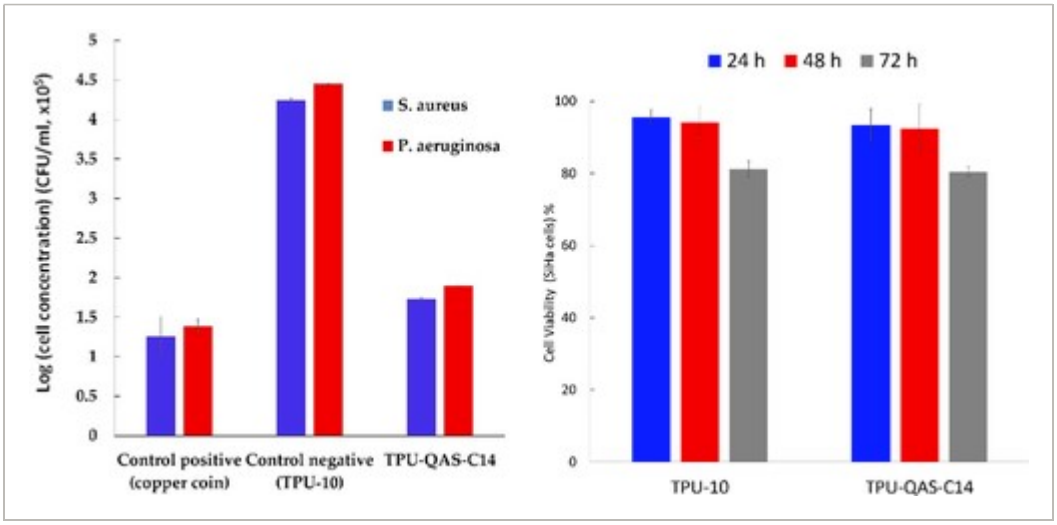

FIGURE 8

Open in figure viewer | PowerPoint

Antibacterial activity of a copper coin (control), TPU-10, and TPU-QAS-C_{14} against *S. aureus* and *P. aeruginosa* bacteria (left). Percentage of cell viability of SiHa cells after being exposed 24, 48, and 72 h to TPU-10 and TPU-QAS-C_{14} (right) [Color figure can be viewed at wileyonlinelibrary.com]

3.4 Synthetic procedure of TPU-QAS-C_{14}

The preparation of a TPU incorporating the QAS active moiety was carried out in two steps following the procedure described for the formation of TPU-10 (Table 3). In that case, QAS-C_{14} was introduced in the second step of the reaction using only 0.5 mol% compared to the other reagents. This small quantity of ammonium salt was expected to confer significant antibacterial properties to the polymeric compound as well as to minimize a potential change of mechanical

properties of the final material. First, TPU-QAS-C_{14} was prepared with a very good yield and the molecular weight reached 30 kDa (Table 3). The ^{1}H-NMR spectrum attests to the successful polymerization (Figure S3).

TABLE 3. TPU-10 and TPU-QAS-C_{14} compositions, yields, and M_n

Compounds	TPUs composition PTHF/MDI/BDO/QAS (molar ratio)				Yield (%)	M_n (kDa)
	MDI	PTHF	BDO	QAS		
TPU-10	4.4	1	3	0	90	38
TPU-QAS-C_{14}	4.4	1	2.96	0.04	91	30

As far as the physical properties are concerned, we can note a slight increase of T_g from −35 to −15°C in going from TPU-10 to TPU-QAS-C_{14}, respectively, while the T_m followed the opposite trend decreasing from 189 to 156°C for TPU-10 to TPU- QAS-C_{14}, respectively (Table 4). However, the DMTA analysis revealed only minor variations of storage and loss modulus, values decreasing from 196 and 31 MPa to 192 and 29 MPa for TPU-10 and TPU-QAS-C_{14}, respectively. Taking into consideration the low amount of the incorporated QAS (0.5 mol%), no significant changes were observed between the two samples. Fortunately, the modified TPU reserved its thermal and thermo-mechanical properties.

TABLE 4. TGA, MDSC, DMTA, and contact angle values of TPU-10 and TPU-QAS-C_{14}

Sample	T_d (°C)	T_o (°C)	T_g (°C)	T_m (°C)	E' (MPa)	E'' (MPa)	Contact angle (°)
TPU-10	273/419/492	254	−35	189	196	31	80 ± 0.8
TPU-QAS-C_{14}	330/430/570	220	−15	156	192	29	93 ± 0.3

In wettability studies, surfaces are divided into two categories. Surfaces that yield water contact angles less than 90° are estimated as more hydrophilic and those higher than 90° are hydrophobic.[74] Here, a contact angle experiment highlighted a more hydrophobic character for TPU-QAS-C_{14} compared to TPU-10. This behavior could be attributed to the long alkyl chain of the QAS-C_{14} unit although only 0.5 mol% were used. Ming Li et al. studied the influence of increased QAS carbon chain length on the antibacterial efficiency of nanocellulose-based material with quaternary ammonium groups, where an increase of chain length from 8 to 18

carbons led to an increase in the contact angle from 80 to 140°. They explained that the groups with a longer carbon chain exhibited a hydrophobic segment that played a serious role during the process of killing the bacterial.[75]

3.5 Biological tests

3.5.1 Minimum inhibitory concentration determination of QAS-C_{14}

To verify the antibacterial activity of QAS-C_{14}, its MIC was determined against Gram-positive *S. aureus* and Gram-negative *P. aeruginosa*. QAS-C_{14} had a strong antibacterial activity, both on the Gram-positive (MIC of 4 0.88 μg/ml) and the Gram-negative bacteria (MIC of 78 μg/ml), although on the Gram-negative bacteria this activity was 16 times lower. This could be due to the existence of the phospholipid bilayer on the latter one rendering it more difficult to penetrate. As expected, the mechanism of attacking the cell membrane is due to the electrostatic interaction between the positively charged moieties and the negatively charged bacteria. This antibacterial activity was slightly higher compared to previously published results. For example, the antibacterial activity of Gemini quaternary ammonium salts showed a MIC value of 12 μg/ml against *S. aureus* and 90 μg/ml against *P. aeruginosa*.[76]

3.5.2 Contact antibacterial activity of TPU-10 and TPU-QAS-C_{14}

In a second step, we evaluated the antibacterial activity of TPU-QAS-C_{14} compared to TPU-10 and a copper coin as a positive control, in a contact antimicrobial assay. It is worth stressing that the detected incorporated percentage of QAS in the TPU was confirmed to be around 0.6% by ^{1}H-NMR. As the QAS is covalently bonded to the TPU, no inhibition zone was to be expected when testing TPU-QAS-C_{14} as a film. However, a tremendous decrease in the CFU/ml was observed for TPU-QAS-C_{14} compared to TPU-10 confirming the engagement of a high antibacterial property in the modified sample (Figures 8,9). The killing process followed first-order kinetics as known from protocols such as ISO 22196 and JIS Z 2801, therefore an antibacterial activity is defined as a decrease of 2 $\log_{10}$ units of a bacterial suspension (10^5 bacteria/ml).[77] This antibacterial polymeric material performed thus well either in the 5 min. Contact with the inoculum or/and in the following 24 h biofilm growth condition (compared to the most efficient antibacterial materials used for biomedical applications.[78-80]

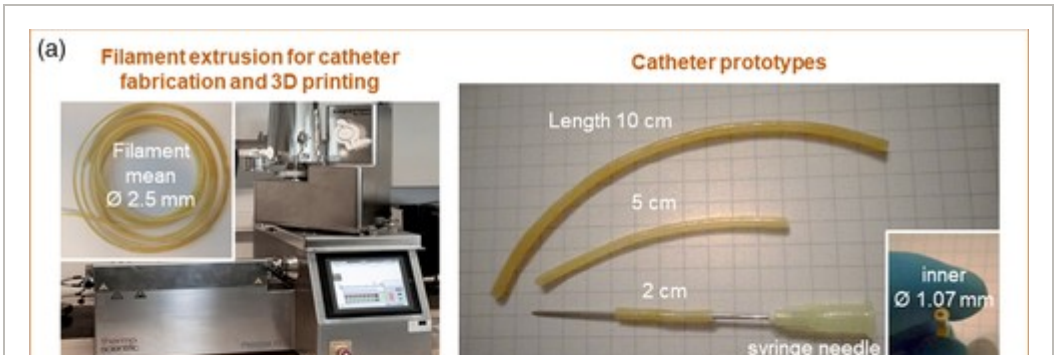

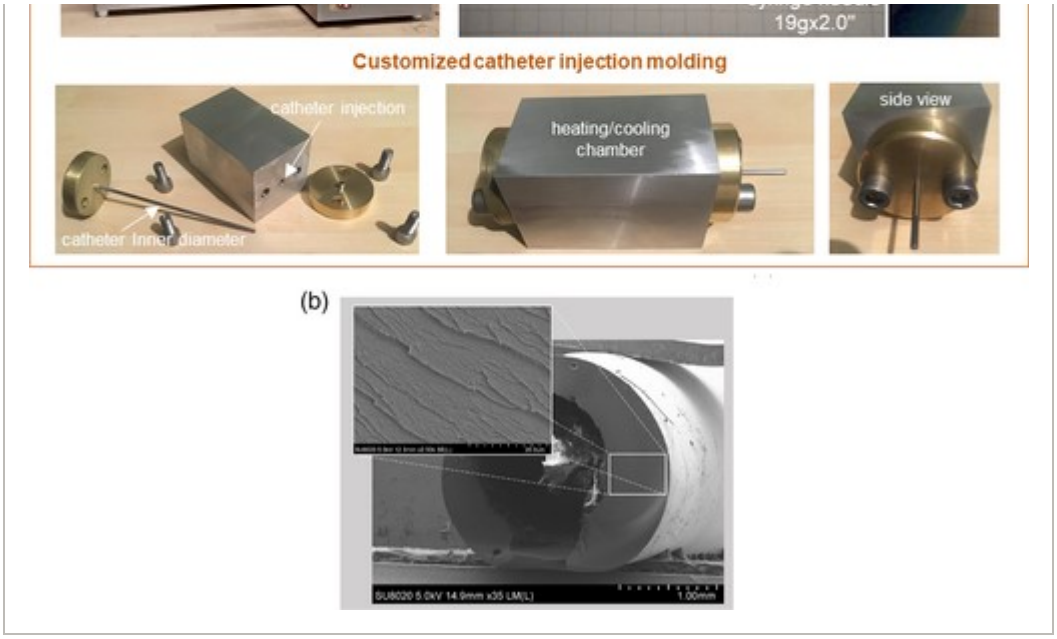

FIGURE 9

Open in figure viewer | PowerPoint

Example of TPU-QAS-C_{14} catheter fabrication using extrusion process approach or customized injection molding (a) and SEM micrograph of the extruded catheter (b) [Color figure can be viewed at wileyonlinelibrary.com]

3.5.3 IC_{50} determination of dissolved TPU-10 and TPU-QAS-C_{14}

The cytotoxicity of TPU-10 and TPU-QAS-C_{14} (dissolved in DMSO) was evaluated in an MTT assay after 24, 48, and 72 h of incubation. The results of the cytotoxicity assay on the human epithelial SiHa cell line showed a dose-dependent decrease in viability in the presence of both dissolved polymers (Table 5). It is worth mentioning that cationic carriers exhibit a toxic effect on cells. They tend to disturb the cell membrane integrity and decrease their metabolic activity. Therefore, a low amount of charged groups are advised to be incorporated in polymers for the sake of cytocompatibility.[81-83] IC_{50} values were indeed low (16.77 and 17.78 mg/ml for TPU-10 and TPU-QAS-C_{14}, respectively), confirming that the synthesized compounds are toxic to the cells. However, when incorporated in a polymer this cytotoxicity could disappear. Therefore, a cytotoxicity study on the polymer (in a solid form) was performed.

TABLE 5. Evaluation of the cell viability (in %) and IC_{50} of the synthesized DMSO dissolved TPU-10 and TPU-QAS-C_{14} polymers at different concentrations

Polymer concentration in DMSO (µg/ml)	Cell viability (%)	
	TPU-10	TPU-QAS-C_{14}
0.125	84	88

Polymer concentration in DMSO (µg/ml)	Cell viability (%)	
	TPU-10	TPU-QAS-C_{14}
0.25	82	87
0.5	80	86
1	74	83
2	69	79
4	61	65
8	56	57
16	43	42
32	32	31

3.5.4 Cytotoxicity activity of TPU-10 and TPU-QAS-C_{14}

The cytotoxic effect of TPU-10 and TPUs-QAS-C_{14} films was also investigated on the human epithelial SiHa cell line after 24 h pre-incubation in cell culture medium and for 24, 48, or 72 h cell exposure, in agreement with ISO 10993-5. The SiHa cell line is a very common human epithelial cell line, such as the HeLa cell line. They are both obtained from cervical cancer patients, being transformed by high-risk papillomavirus (HPV-16 in the case of the SiHa cells). They have a doubling generation time as most cell lines, being around 20 h, and are adherent as expected from an epithelial cell line. So, they are considered as a useful tool to study the impact of compounds on the viability of adherent epithelial cells derived from mucosal epithelia (cervical epithelia in this case).[84] The % cell viability after the exposure was determined in an MTT assay by comparing sample well viability with control well viability. Polymeric materials are usually defined as nontoxic when cell viability is maximally reduced by 10%, as slightly cytotoxic when cell viability reached between 60% and 90%, as moderately cytotoxic when cell viability reached between 30% and 60%, and as severely cytotoxic when cell viability is less than 30%.[85]

The amount of formazan produced by SiHa cells exposed to the samples decreased slightly after 24 and 48 h compared to the control. After 72 h, the % cell viability reached ~80% without a significant difference between samples. The synthesized samples showed slight cytotoxicity that seems to be in the acceptable range for biomedical application as compared to other biomaterials.[86, 87] Having the QAS covalently bonded to the polymer and in a very low

percentage probably helped to maintain low cytotoxicity, leading to a safe material for biomedical applications.

3.6 Catheter fabrication

Finally, the catheter fabrication was performed through extrusion (process 11 parallel twin-screw extruder) by first producing a filament with the desired diameter (2.5 mm) and length of several tens of centimeters, as shown in Figure 9(a). The morphological studies of the catheter, revealed a homogenous polymer matrix (absence of air bubbles of fractures), confirming the stability of the material fabrication as evidenced by the SEM micrographs (Figure 9(b)). The advantage of this approach is that the obtained filament presented a regular diameter along its length, without enclosed air bubbles and thermo-oxidative degradation of the TPUs material (preservation of the material color). As a second step, the filament was subjected to perfusion to create a series of catheters with different lengths and an inner diameter of 1.07 mm. In addition, a customized catheter injection molding approach was also developed, proposing a fast one-step production approach of single catheters with various inner diameters. The developed biomaterials present promising biomedical application as a catheter, with suitable mechanical and antibacterial properties. They can be tested in human blood test protocols to evaluate the blood cell adhesion on the inner diameter wall of the device, as well as the coagulation impact of the TPU on the blood properties by performing thromboelastographic tests (blood prothrombin time and activated partial thromboplastin time). In addition, the great potential of the additive manufacturing techniques can be explored by using the TPUs filament for the fabrication of biomedical devices with desirable shapes and properties by fused deposition modeling 3D printing technique.

4 CONCLUSIONS

In summary, this work has consisted of the determination of the best condition for the fabrication of biocompatible PU-based materials with well-defined mechanical properties targeting biomedical applications, such as catheters. It was found that both the working temperature and the quantity of MDI, played a crucial role in the fabrication of TPUs with the desired physio-mechanical properties. In a second step, the design of a polymeric compound endowed with antibacterial activities was performed. For this, a QAS-C_{14} was successfully synthesized and its high antibacterial properties against both Gram-positive *S. aureus* and Gram-negative *P. aeruginosa* were confirmed. Subsequently, the incorporation of about 0.5 mol% of QAS-C_{14} in TPU-QAS-C_{14} gave rise to a series of TPUs biomaterials with pronounced antibacterial properties and low cytotoxicity effect, while preserving the final materials mechanical strength. In addition, first catheter prototypes were developed revealing the great potential of the study in the biomedical aspect, as well as in the creation of next-generation biomedical devices through innovative additive manufacturing approaches –

FDM-3D printing or customized injection molding.

ACKNOWLEDGMENTS

The research was financially supported by the PROSTEM Project, the COST Action CA15114 "AMiCI" (Antimicrobial Coating Innovations to Prevent Infectious Diseases) and the COST action TD1305 "iPROMEDAI" (Improved PROtection of MEdical Devices Against Infection). SMPC is grateful to the Region Wallonne support in the case of LCFM-BIOMAT and Jean-Marie Raquez is a senior research associate at FRS-FNRS.

Supporting Information

Filename	Description
app51666-sup-0001-Supinfo.docx Word 2007 document , 965.1 KB	**Appendix S1**: Supporting Information.

Please note: The publisher is not responsible for the content or functionality of any supporting information supplied by the authors. Any queries (other than missing content) should be directed to the corresponding author for the article.

REFERENCES

1 J. O. Akindoyo, M. D. H. Beg, S. Ghazali, M. R. Islam, *RSC Adv.* 2016, **6**, 453.
Crossref | Web of Science® | Google Scholar

2 O. Bayer, *Angew. Chemie* 1947, **59**, 257.
Wiley Online Library | CAS | Web of Science® | Google Scholar

3 G. Wegener, M. Brandt, L. Duda, B. Klesczewski, D. Koch, R. Kumpf, H. Orzesek, H. Pirkl, C. Six, C. Steinlein, M. Weisbeck, *Appl. Catal. Gen.* 2001, **221**, 303.
Crossref | CAS | Web of Science® | Google Scholar

4 D. Xie, X. Zhang, *J. Mater. Sci.* 2014, **49**, 7339.
Crossref | Web of Science® | Google Scholar

5 L. Xu, M. E. Meyerhoff, C. A. Siedlecki, *Acta Biomater.* 2019, **84**, 77.
Crossref | CAS | PubMed | Web of Science® | Google Scholar

6 J. A. Lichter, M. F. Rubner, *Langmuir* 2009, **25**, 295.
Crossref | Web of Science® | Google Scholar

7 H. Ren, J. L. Bull, M. E. Meyerho, *ACS Biomater Sci. Eng.* 2016, **2**, 1483.
Crossref | CAS | PubMed | Web of Science® | Google Scholar

8 P. Król, B. Król, *J. Mater. Sci.* 2020, **55**, 73.
Crossref | CAS | Web of Science® | Google Scholar

9 M. A. Sawpan, *J. Polym. Res.* 2018, **25**, 109.
Crossref | Web of Science® | Google Scholar

10 M. Ghasemlou, F. Daver, E. P. Ivanova, B. Adhikari, *Ind. Crops Prod.* 2019, **142**, 841.
Crossref | Web of Science® | Google Scholar

11 A. Agrawal, R. Kaur, R. S. Walia, *Eur. Polym. J.* 2017, **95**, 255.
Crossref | CAS | Web of Science® | Google Scholar

12 A. Tenorio-alfonso, M. C. Sánchez, J. M. Franco, *J. Polym. Environ.* 2020, **28**, 749.
Crossref | CAS | Web of Science® | Google Scholar

13 G. Matthijs, *Polym. Int.* 2019, **68**, 843.
Wiley Online Library | Web of Science® | Google Scholar

14 D. Naldzhiev, D. Mumovic, M. Strlic, *Build. Environ.* 2019, **169**, 559.
Google Scholar

15 C. Chaves, F. Alshomer, R. G. Palgrave, D. M. Kalaskar, U. P. Sud, O. Surgery, H. Antoine, *ACS Applied Materials & Interfaces* 2016, **29**, 701.
Google Scholar

16 L. S. Dandeniyage, R. Adhikari, M. Bown, R. Shanks, B. Adhikari, C. D. Easton, T. R. Gengenbach, D. Cookson, P. A. Gunatillake, *J. Biomed. Mater. Res.* 2018, **107**, 112.
Wiley Online Library | Web of Science® | Google Scholar

17 E. M. Christenson, M. Dadsetan, M. Wiggins, J. M. Anderson, A. Hiltner, *J. Biomed. Mater. Res. A* 2004, **69**, 407.
Wiley Online Library | CAS | PubMed | Web of Science® | Google Scholar

18 A. Simmons, J. Hyvarinen, R. A. Odell, D. J. Martin, P. A. Gunatillake, K. R. Noble, L. A. Poole-warren,

Biomaterials 2004, **25**, 4887.
Crossref | CAS | PubMed | Web of Science® | Google Scholar

19 B. F. D'Arlas, L. Rueda, K. De la Caba, I. Mondragon, A. Eceiza, *Polym. Eng. Sci.* 2008, **48**, 519.
Wiley Online Library | CAS | Web of Science® | Google Scholar

20 R. Hernandez, J. Weksler, A. Padsalgikar, J. Runt, *J. Biomed. Mater.* 2008, **87**, 546.
Wiley Online Library | CAS | PubMed | Web of Science® | Google Scholar

21 S. Saint, M. T. Greene, S. L. Krein, M. A. Rogers, D. Ratz, K. E. Fowler, B. S. Edson, S. R. Watson, B. Meyer-Lucas, M. N. Masuga, *Engl. J. Med.* 2016, **374**, 2111.
Crossref | CAS | PubMed | Web of Science® | Google Scholar

22 M. Gominet, F. Compain, C. Beloin, D. Lebeaux, *APMIS* 2017, **125**, 365.
Wiley Online Library | CAS | PubMed | Web of Science® | Google Scholar

23 R. Leistner, E. Hirsemann, A. Bloch, P. Gastmeier, C. Geffers, *Infection* 2014, **42**, 31.
Crossref | CAS | PubMed | Web of Science® | Google Scholar

24 R. Gahlot, C. Nigam, V. Kumar, G. Yadav, S. Anupurba, *Int. J. Crit. Illn. Inj. Sci.* 2014, **4**, 162.
Crossref | PubMed | Google Scholar

25 K. G. Neoh, M. Li, E.-T. Kang, E. Chiong, P. A. Tambyah, *J. Mater. Chem. B* 2017, **5**, 2045.
Crossref | CAS | PubMed | Web of Science® | Google Scholar

26 S. Mahira, A. Jain, W. Khan, A. J. Domb, *Antimicrobial Materials for Biomedical Applications*, Royal Society of Chemistry, UK 2019, p. 1.
Crossref | Google Scholar

27 D. Filip, D. Macocinschi, M. Fernanda, Z. Cristian, D. Varganici, *Polym. Bull.* 2018, **75**, 701.
Crossref | CAS | Web of Science® | Google Scholar

28 B. W. Chua, C. S. Lee, *J. Appl. Polym. Sci.* 2018, **135**, 6045.
Wiley Online Library | Web of Science® | Google Scholar

29 B. Pant, M. Park, S. Park, *Polymers* 2019, **11**, 1185.
Crossref | CAS | Web of Science® | Google Scholar

30 S. Heilman, L. G. A. Silva, *J. Nanopart. Res.* 2017, **47**, 17.
Crossref | CAS | Web of Science® | Google Scholar

31 R. Ciceo Lucacel, T. Radu, A. S. Tătar, I. Lupan, O. Ponta, *J. Non. Cryst. Solids* 2014, **404**, 98.
Crossref | CAS | Web of Science® | Google Scholar

32 J. Jiang, Y. Fu, Q. Zhang, X. Zhan, C. Fengqiu, *Appl. Surf. Sci.* 2017, **412**, 1.
Crossref | CAS | Web of Science® | Google Scholar

33 K. Yu, J. C. Y. Lo, M. Yan, X. Yang, D. E. Brooks, R. E. W. Hancock, D. Lange, J. N. Kizhakkedathu, *Biomaterials* 2017, **116**, 69.
Crossref | CAS | PubMed | Web of Science® | Google Scholar

34 S. Wendels, L. Avérous, *Bioact. Mater.* 2021, **6**, 1083.
Crossref | CAS | PubMed | Web of Science® | Google Scholar

35 A. Fonseca, P. Morais, R. Branco, A. Serra, J. Coelho, P. Mendonça, M. Santos, *Materials* 2016, **9**, 599.
Crossref | Web of Science® | Google Scholar

36 Y. Jiao, L. Niu, S. Ma, J. Li, F. R. Tay, J. Chen, *Prog. Polym. Sci.* 2017, **71**, 53.
Crossref | CAS | PubMed | Web of Science® | Google Scholar

37 S. Zanini, A. Polissi, E. A. Maccagni, E. C. Dell'Orto, C. Liberatore, C. Riccardi, *J. Colloid Interface Sci.* 2015, **451**, 78.
Crossref | CAS | PubMed | Web of Science® | Google Scholar

38 L. Li, H. Zhou, F. Gai, X. Chi, Y. Zhao, F. Zhang, Z. Zhao, *RSC Adv.* 2017, **7**, 244.
Google Scholar

39 B. Gao, Q. Liu, Y. Li, *J. Polym. Environ.* 2010, **18**, 474.
Crossref | CAS | Web of Science® | Google Scholar

40 J. Wang, Q. Mei, L. Lin, F. Sun, J. Li, Q. Zou, Y. Zuo, *RSC Adv.* 2019, **9**, 7043.
Crossref | CAS | Web of Science® | Google Scholar

41 M. Sánchez-Adsuar, E. Papon, J.-J. Villenave, *J. Appl. Polym. Sci.* 1999, **76**, 1590.
Wiley Online Library | Web of Science® | Google Scholar

42 M. Xiao, N. Zhang, J. Zhuang, Y. Sun, F. Ren, W. Zhang, *Polymers* 2019, **11**, 1002.
Crossref | CAS | Web of Science® | Google Scholar

43 S. Markossian, A. Grossman, K. Brimacombe, M. Arkin, D. Auld, C. Austin, J. Baell, T. Chung, N.

Coussens, J. Dahlin V. Devanarayan, T. Foley, M. Glicksman, M. Hall, J. Haas, S. Hoare, J. Inglese, P. Iversen, S Kales, M. Lal-Nag, Z. Li, J. McGee, O. McManus, T. Riss, P. Saradjian, G. Sittampalam, M. Tarselli, O. J J. Trask, Y. Wang, J. Weidner, M. Wildey, K. Wilson, M. Xia, X. Xu. Assay Guidance Manual; Bethesda (MD): Eli Lilly & Company and the National Center for Advancing Translational Sciences, 2004.
Google Scholar

44 J. L. Ã. Sebaugh, *Pharm. Stat.* 2011, **10**, 128.
Wiley Online Library | CAS | PubMed | Web of Science® | Google Scholar

45 In ISO 10993-5:2009 Biological evaluation of medical devices; American National Standards Institute (ANSI), 2009; p 34.
Google Scholar

46 C. Prisacariu, E. Scortanu, *High Perform. Polym.* 2011, **23**, 308.
Crossref | CAS | Web of Science® | Google Scholar

47 A. Lowe, J. M. Buist, *Ann. Occup. Hyg.* 1965, **8**, 143.
Google Scholar

48 M. J. T. Raaijmakers, N. E. Benes, *Prog. Polym. Sci.* 2016, **63**, 86.
Crossref | CAS | Web of Science® | Google Scholar

49 M. Szycher, *J. Am. Chem. Soc.* 2000, **16**, 3983.
Google Scholar

50 S. Wendels, T. Chavez, M. Bonnet, K. A. Salmeia, S. Gaan, *Materials* 2017, **10**, 784.
Crossref | Web of Science® | Google Scholar

51 H. Park, H. You, H. Jo, I. Shim, *J. Coat Technol. Res.* 2006, **3**, 53.
Crossref | CAS | Web of Science® | Google Scholar

52 T. A. Speckhard, K. K. S. Hwang, S. L. Cooper, V. S. C. Chang, J. P. Kennedy, *Polymer (Guildf)* 1985, **26**, 70.
Crossref | CAS | Web of Science® | Google Scholar

53 B. Willocq, J. Odent, P. Dubois, J.-M. Raquez, *RSC Adv.* 2020, **10**, 766.
Crossref | Web of Science® | Google Scholar

54 S. L. Cooper, J. Guan, *Advances in Polyurethane Biomaterials*, Woodhead Publishing, UK 2016.
Google Scholar

55 Y. Li, W. Kang, *Macromolecules* 1994, **27**, 612.
Crossref | CAS | Web of Science® | Google Scholar

56 M. Barikani, M. V. E. Seyed, M. SM, *Polym. Plast. Technol. Eng* 2007, **46**, 1087.
Crossref | CAS | Web of Science® | Google Scholar

57 D. J. Hourston, G. Williams, R. Satguru, J. D. Padget, D. Pears, *J. Appl. Polym. Sci.* 1997, **66**, 2035.
Wiley Online Library | CAS | Web of Science® | Google Scholar

58 E. Sharmin, F. Zafar, *Polyurethane*, Intechopen, Croatia 2012, p. 3.
Google Scholar

59 R. Morales-cerrada, R. Tavernier, S. Caillol, *Polymers* 2021, **13**, 1255.
Crossref | CAS | PubMed | Web of Science® | Google Scholar

60 S. Yeong-tarng, H. Chen, K. Liu, Y. Twu, *J. Polym. Sci. Part A Polym. Chem.* 1999, **37**, 4126.
Wiley Online Library | Web of Science® | Google Scholar

61 S. Murata, T. Izumi, H. Ito, *Polymers* 2012, **60**, 593.
CAS | Google Scholar

62 M. C. Kuo, S. M. Shau, J. M. Su, R. J. Jeng, T. Y. Juang, S. A. Dai, *Macromolecules* 2012, **45**, 5358.
Crossref | CAS | Web of Science® | Google Scholar

63 C. H. Wu, S. M. Shau, S. C. Liu, S. A. Dai, S. C. Chen, R. H. Lee, C. F. Hsieh, R. Jeng, *J. RSC Adv.* 2015, **5**, 897.
Google Scholar

64 F. Xie, T. Zhang, P. Bryant, V. Kurusingal, J. M. Colwell, B. Laycock, *Prog. Polym. Sci.* 2019, **90**, 211.
Crossref | CAS | Web of Science® | Google Scholar

65 M. Villani, R. Consonni, M. Canetti, F. Bertoglio, S. Iervese, G. Bruni, L. Visai, S. Iannace, F. Bertini, *Polymers* 2020, **12**, 362.
Crossref | CAS | Web of Science® | Google Scholar

66 T. Calvo-correas, M. D. Martín, A. Retegi, N. Gabilondo, M. A. Corcuera, A. Eceiza, *ACS Sustainable Chem. Eng.* 2016, **4**, 5684.
Crossref | CAS | Web of Science® | Google Scholar

67 A. K. Barick, D. K. Tripathy, *J. Appl. Polym. Sci.* 2010, **117**, 639.

Wiley Online Library | CAS | Web of Science® | Google Scholar

68 M. Asensio, V. Costa, *Polymers* 2019, **11**, 1.
Crossref | Web of Science® | Google Scholar

69 M. Razmara, S. H. Saidpour, S. Arunchalam, presented at Int. Conf. Fascin. Adv. Mech. Eng., 11–13 December 2008.
Google Scholar

70 D. Lee, H. Tsai, R. Tsai, P. H. Chen, *Polym. Eng. Sci.* 2007, **47**, 695.
Wiley Online Library | CAS | Web of Science® | Google Scholar

71 P. Alves, J. F. J. Coelho, J. Haack, A. Rota, A. Bruinink, M. H. Gil, *Eur. Polym. J.* 2009, **45**, 1412.
Crossref | CAS | Web of Science® | Google Scholar

72 M. Sáenz-Pérez, E. Lizundia, J. M. Laza, J. García-Barrasa, J. L. Vilasa, L. M. León, *RSC Adv.* 2016, **6**, 1.
Crossref | Web of Science® | Google Scholar

73 B. C. Bovas, L. Karunamoorthy, F. B. Chuan, *Mater. Res. Exp.* 2020, **6**, 6.
Google Scholar

74 K. Y. Law, *J. Phys. Chem. Lett.* 2014, **5**, 686.
Crossref | CAS | PubMed | Web of Science® | Google Scholar

75 M. Li, X. Liu, N. Liu, Z. Guo, P. K. Singh, S. Fu, *Colloids Surfaces A* 2018, **554**, 122.
Crossref | CAS | Web of Science® | Google Scholar

76 A. Piecuch, K. Guz-regner, E. Dworniczek, *FEMS Microbiol. Lett.* 2014, **350**, 190.
Wiley Online Library | PubMed | Web of Science® | Google Scholar

77 D. Pei, J. Wang, Y. Mu, X. Wan, *Macromol. Chem. Phys.* 2017, **203**, 1.
Google Scholar

78 Z. Liu, C. Chen, R. Jiang, J. Zhao, L. Ren, *Mater. Lett.* 2021, **286**, 186.
Google Scholar

79 A. Hasanzadeh, B. Gholipour, S. Rostamnia, A. Eftekhari, A. Tanomand, *J. Colloid Interface Sci.* 2021, **585**, 676.
Crossref | CAS | PubMed | Web of Science® | Google Scholar

80 D. Cai, X. Zhao, L. Yang, R. Wang, G. Qin, *J. Mater. Sci. Technol.* 2021, **81**, 13.
Crossref | Web of Science® | Google Scholar

81 D. Fischer, Y. Li, B. Ahlemeyer, J. Krieglstein, T. Kissel, *Biomaterials* 2003, **24**, 1121.
Crossref | CAS | PubMed | Web of Science® | Google Scholar

82 T. R. Stratton, J. L. Rickus, J. P. Youngblood, *Biomacromolecules* 2009, **10**, 2550.
Crossref | CAS | PubMed | Web of Science® | Google Scholar

83 T. R. Stratton, J. A. Howarter, B. C. Allison, B. M. Applegate, J. P. Youngblood, *Biomacromolecules* 2010, **11**, 1286.
Crossref | CAS | PubMed | Web of Science® | Google Scholar

84 J. D. Meissner, J. Gen, *Virology* 1725, **1999**, 80.
Google Scholar

85 F. Norouz, R. Halabian, A. Salimi, M. Ghollasi, *Mater. Sci. Eng. C* 2019, **103**, 9857.
Crossref | Web of Science® | Google Scholar

86 S. Miao, L. Sun, P. Wang, R. Liu, Z. Su, S. Zhang, *Eur. J. Lipid Sci. Technol.* 2012, **114**, 1165.
Wiley Online Library | CAS | Web of Science® | Google Scholar

87 S. Guelcher, A. Srinivasan, A. Hafeman, K. Gallagher, J. Doctor, S. Khetan, S. M. C. Bride, J. Hollinger, *Tissue Eng.* 2007, **13**, 2321.
Crossref | CAS | PubMed | Web of Science® | Google Scholar